Molecular and Cellular Neuroscience 127 (2023) 103900

Contents lists available at ScienceDirect

Molecular and Cellular Neuroscience

journal homepage: www.elsevier.com/locate/ymcne

Efferent axons in the zebrafish lateral line degenerate following sensory hair cell ablation

Melek Umay Tuz-Sasik, Remy Manuel, Henrik Boije *

Department of Immunology, Genetics and Pathology, Cell and Neurobiology, Uppsala University, Uppsala, Sweden

ARTICLE INFO

Keywords:
Regeneration
Sensory afferent
Neomycin
*atoh1*a
Danio rerio

ABSTRACT

The zebrafish lateral line is a frequently used model to study the mechanisms behind peripheral neuronal innervation of sensory organs and the regeneration thereof. The lateral line system consists of neuromasts, a cluster of protruding hair cells, which are innervated by sensory afferent and modulatory efferent neurons. These flow-sensing hair cells are similar to the hair cells in the mammalian ear. Though, while hair cell loss in humans is irreversible, the zebrafish neuromasts are regarded as the fastest regenerating structure in vertebrates, making them an ideal model to study regeneration. However, one component of the lateral line system, the efferent projections, has largely been omitted in regenerative studies. Here, for the first time, we bring insights into the fate of efferent axons during ablation and regeneration of the hair cells in the zebrafish lateral line. Our behavioral analysis showed functional recovery of hair cells and sensory transmission within 48 h and their regeneration were in line with previous studies. Analysis of the inhibitory efferent projections revealed that in approximately half the cases the inhibitory efferent axons degenerated, which was never observed for the sensory afferent axons. Quantification of hair cells following ablation suggests that the presence of mature hair cells in the neuromast may prevent axon degeneration. Within 120 h, degenerated efferent axons regenerated along the axonal tract of the lateral line. Reanalysis of published single cell neuromast data hinted to a role for Bdnf in the survival of efferent axons. However, sequestering Bdnf, blocking the Trk-receptors, and inhibiting the downstream ERK-signaling, did not induce axon degeneration, indicating that efferent survival is not mediated through neurotrophic factors. To further explore the relation between hair cells and efferent projections, we generated *atoh1a* mutants, where mature hair cells never form. In larvae lacking hair cells, inhibitory efferent projections were still present, following the tract of the sensory afferent without displaying any innervation. Our study reveal the fate of efferent innervation following hair cell ablation and provide insights into the inherent differences in regeneration between neurons in the peripheral and central nervous system.

1. Introduction

Regeneration has great value for medical therapy and while all vertebrates possess the ability to heal damaged tissues, the capacity varies between tissues and among species. For instance, non-mammalian vertebrates possess a greater ability to regenerate than mammals (Tsonis, 2000) and regeneration of the peripheral nervous system is substantially more robust than in the central nervous system (Pleasure, 1999). Understanding the underlying mechanisms in different contexts may provide insights into how regeneration can be triggered in regions with inherent poor capacity, such as the human central nervous system.

In humans, damage of mechanosensory hair cells in the inner ear leads to hearing loss, resulting in permanent impairment due to their inability to regenerate. The flow-sensing hair cells in the lateral line display great similarity to the hair cells in the mammalian ear and there are several zebrafish models to study human hearing disorders (Whitfield, 2002). Furthermore, drug discovery studies have aimed to prevent hair cell loss or stimulate regeneration in zebrafish (Coffin et al., 2010; Ou et al., 2010). The lateral line is unique to fish and amphibians and is comprised of superficial organs called neuromasts, which contain

Abbreviations: REN, rostral efferent nucleus; CEN, caudal efferent nucleus; RELL, rhombencephalic efferent neuron to the lateral line; DELL, diencephalic efferent of the lateral line; dpf, days post fertilization; hpt, hours post treatment; *bdnf*, *brain derived neurotrophic factor*; *ngf*, *nerve growth factor*; *ntf3*, *neurotrophin factor 3*; *nt4/5*, *neurotrophin 4/5*; *nt6/7*, *neurotrophin 6/7*.

* Corresponding author.
E-mail address: henrik.boije@igp.uu.se (H. Boije).

https://doi.org/10.1016/j.mcn.2023.103900
Received 6 July 2023; Received in revised form 5 September 2023; Accepted 7 September 2023
Available online 13 September 2023

protruding hair cells. These neuromasts help aquatic animals to detect changes in water flow (Ghysen and Dambly-Chaudière, 2004). As water pass over the animal, stereocilia are deflected towards the kinocilium, causing a release of glutamate to sensory afferent neurons innervating the hair cells (Pichler and Lagnado, 2019). These sensory afferent neurons, with somas located in two ganglia, relay the information to the brain (Vanwalleghem et al., 2020). In zebrafish, this sensory system is modulated by efferent neurons located in three brain nuclei: the diencephalic efferent of the lateral line (DELL; excitatory efferent neurons) located in the diencephalon, the rostral efferent nucleus (REN), and the caudal efferent nucleus (CEN), found in the rhombencephalon (both inhibitory efferent neurons; Bricaud et al., 2001). We thus have a relatively simple system to study the regeneration of a sensory organ alongside the peripheral and central neurons involved in relaying and modulating the input. The zebrafish neuromasts have been regarded as the fastest regenerating structure in vertebrates, with the first newly generated hair cells in around 5 h (Baek et al., 2022). While there are many studies regarding the regeneration of hair cells (Baek et al., 2022; Lush and Piotrowski, 2014; Venuto and Erickson, 2021) and sensory afferent projections (Hardy et al., 2021; Lush and Piotrowski, 2014), there is no information regarding the fate of efferent axons during these events. Revealing the fate of efferent projections during regeneration of the lateral line could offer insights into differences in regenerative capacity observed in neurons of the peripheral and central nervous system. Moreover, it may advance the zebrafish as a model for studies regarding deafness in humans.

Using transgenic zebrafish to label efferent neurons of the lateral line (Manuel et al., 2021), we describe the fate of their axons following hair cell ablation. Behavioral recovery and regeneration of hair cells and sensory innervation was observed within 48 h, in line with previous findings. Strikingly, while both sensory afferent and inhibitory efferent projections showed reduced neuromast innervation following hair cell ablation, efferent projections degenerated in approximately 50 % of the cases. Regeneration and reinnervation by degenerated efferent projections occurred within 120 h, indicating that the efferent neurons did not undergo apoptosis. Quantification of mature hair cells following ablation suggests that their rapid reemergence is required to prevent efferent axon degeneration. Although Bdnf emerged as a candidate, it does not appear to govern the survival of efferent axons. Using *atoh1a* crispants, which are unable to generate mature hair cells, we found inhibitory efferent axons along the lateral line but these did not innervate the neuromast. We conclude that efferent axons, once synapsed onto a mature hair cell, likely become dependent on an unknown survival cue secreted by the mature hair cells. In all, we show that insult to a sensory organ results in divergent responses for afferent and efferent axons, a phenomenon that may affect human medical conditions.

2. Material and methods

2.1. Animals and housing

Adult zebrafish were housed at the Genome Engineering Zebrafish National Facility (Uppsala, Sweden) under standard conditions of 14/10 h day/night cycles at 28 °C. Embryos and larvae were kept under constant darkness at 28 °C, in filtrated and UV-treated system water supplemented with 0.5 % methylene blue. Larvae older than 7 days post fertilization (dpf) were fed with rotifers. Embryos for behavioral experiments were obtained from group breeding of wildtype AB. For imaging sessions after neomycin treatment, the following transgenic lines were used: Tg(*dmrt3a*:GAL4) (Satou et al., 2020), Tg(HGn39D) (Faucherre et al., 2009), Tg(*myo6b*:hs:eGFP) (generated for this study), Tg (UAS:eGFP), and Tg(UAS:Tomato). The expression of Tomato was mosaic, likely due to random silencing of its UAS repeats (Akitake et al., 2011). To prevent pigmentation, 1-Phenyl-2-thiourea (PTU, 0.003 % final concentration) was added at 24 h post fertilization (hpf). To generate *atoh1a* crispants, one-cell stage embryos were obtained from group breeding of Tg(*dmrt3a*:GAL4;UAS:eGFP). Appropriate ethical approvals were obtained from a local ethical board in Uppsala (14088/2019).

2.2. Generation of Tg(myo6b:hs:eGFP) zebrafish

2.2.1. sgRNA synthesis

To create a Tg(*myo6b*:hs:eGFP) line, labelling the hair cells in neuromasts, we inserted a plasmid containing eGFP driven by a minimal heat shock promoter upstream of the 5UTR of *myo6b* (ENSDARG00000042141). Using specific sgRNA we targeted DNA 661 base pairs upstream of the start of the 5′UTR of *myo6b* and Cas9 was used to introduce a double strand break. Through nonhomologous end joining the eGFP-plasmid was inserted and its expression regulated by the same machinery as the expression of the gene of interest (Kimura et al., 2014). A CRISPR target was designed using CRISPor and ChopChop; ZNN-18 myo6b GCGACACGTAGTGAGAGATC. Using the oligo assembly approach to prepare sgRNAs (Varshney et al., 2015), we synthetically added a G to the target ZNN-18 GGACACGTAGTGAGAGATC since this is crucial for the T7 polymerase. Oligos were ordered with a T7 promoter 5′ of the target sequence and a DNA stretch overlapping with the guide core sequence at the 3′ end (for ZNN-18 taatacgactcactataGGACACGTAGTGAGAGATCgttttagagctagaaatagcaag). The oligos were then annealed with a second fragment containing the guide core sequence (*i.e.* oligoB) (Varshney et al., 2015). The same principle was used for the oligo to generate the sgRNA to cut the mbait sequence in the plasmid (taatacgactcactataGGCTGCTGCGGTTCCAGAGGgttttagagctagaaatagcaag). These products were then used as a template for RNA *in vitro* transcription (HiScribe T7 High Yield RNA Synthesis Kit, NEB) and the generated RNA was purified prior to injection.

2.2.2. Cas9 mRNA

To prepare Cas9 mRNA, pT3Ts-nCas9 plasmid (Addgene 46757) was digested with Xba1 (NEB), purified and used for T3 driven *in vitro* transcription according to the manual provided by the manufacturer (mMESSAGE m MACHINE T3 Kit, Life Technologies).

2.2.3. Micro-injections

Fertilized zebrafish eggs from AB fish were injected, at the one-cell stage into the cell, with 1 nl final volume [112,5 pg of Cas9 mRNA, 250 pg Cas9 protein (A36498, TrueCut Cas9 Protein v2, Invitrogen, Waltham, MA, USA), 50 pg of sgRNA for gene specific target and 50 pg of mbait sgRNA and 15 pg of the mbait-hs-eGFP plasmid (kindly provided by Professor Atsuo Kawahara (Ota et al., 2016))]. eGFP-positive larvae were raised, outcrossed with AB zebrafish, and offspring were screened for germline transmission.

2.3. Generating atoh1a crispants

2.3.1. sgRNA synthesis

To target *atoh1a* (ENSDARG00000055294), two guide RNAs were prepared based on previously established and tested gRNAs (Navajas Acedo et al., 2019). DNA targeting sgRNA's were as follows: ZNN56 *atoh1a* GGCTGGCTCCCGTGCAGGC and ZNN57 *atoh1a* GGGAGAGGCGAAGAATGCA. Synthesis of the sgRNA was performed as described in the previous paragraph.

2.3.2. Micro-injections

Two nl final volume of the two target-specific gRNAs (120 pg/each), 225 pg of Cas9 mRNA, 500 pg Cas9 protein (A36498, TrueCut Cas9 Protein v2, Invitrogen, Waltham, MA, USA) was injected into one-cell stage embryos. To assess the success of the injections, 5 dpf mutant larvae were stained with DASPEI and screened for a lack of hair cells compared to uninjected control siblings.

2.4. Ablation of hair cells through neomycin sulfate treatment

2.4.1. Whole body treatment

Neomycin sulfate treatment was used to ablate the superficial hair cells as described in our recent publication (Tuz-Sasik et al., 2022). Briefly, free-swimming larvae were exposed to 500 μM neomycin sulfate (PHR1491, Sigma Aldrich, St. Louis, MO, USA) in embryo water for 1 h. Then, the neomycin sulfate solution was replaced with fresh embryo water and larvae were assessed for behavior or used in confocal imaging at various time points following treatment (see Results section for exact timings).

2.4.2. Tail treatment

Similar to whole body treatment, neomycin sulfate treatment was used to ablate the superficial hair cells in only part of the animal. Before treatment, Tg(*dmrt3a*:GAL4;UAS:Tomato) larvae displaying a RELL projection to the tail neuromasts were selected at 4 dpf. The next day, 5 dpf larvae were mounted in 1.2 % low melting agarose solution and embryo water, containing Tricaine (0.12 mg/ml). Agarose covering the larvae between the yolk extension to the tail was removed, leaving only the caudal half of the larvae exposed to the neomycin sulfate solution. After 1 h, larvae were removed from the agarose and the neomycin sulfate solution was replaced with fresh embryo water. Larvae were then used in confocal imaging at various time points following treatment (see Results section for exact timings).

2.5. Staining of hair cells through DASPEI

To visualize hair cells in the neuromasts (Harris et al., 2003), larvae were exposed to the fluorescent dye DASPEI (D0815, Sigma Aldrich, St. Louis, MO, USA). A 25 μg/ml solution was prepared in embryo water and larvae were exposed for 30 min. Larvae were washed twice in embryo water prior to imaging. DASPEI staining of tail treated larvae verified that hair cell ablation only occurred in the exposed region (data not shown).

2.6. Blocking of the Bdnf-Trk pathway

Before treatment, Tg(HGN39D; *dmrt3a*:GAL4;UAS:Tomato) larvae displaying a RELL projection to the tail neuromasts were selected at 4 dpf. Chicken anti-BDNF (200 μg/ml; AF248, R&D Systems, Minneapolis, MN, USA) was used to inhibit Bdnf action through sequestering. PF-06273340 (100 μM; PZ0254, Sigma Aldrich, St. Louis, MO, USA) was used to prevent activation of the TrkA, TrkB, and TrkC receptors. U0126 (100 μM; CST #9903, Cell Signaling Technology, Danvers, MA, USA) was used to block the pan-receptor ERK pathway. Selected larvae were treated overnight (18–21 h) and efferent fate was assessed. Because both U0126 and PF-06273340 were dissolved in DMSO, we supplemented the embryo water for these inhibitors with 2 % DMSO to prevent them from falling out of solution again (Hawkins et al., 2008). Here, control larvae were likewise exposed to 2 % DMSO.

2.7. Behavioral analysis of free-swimming and startle response

A DanioVision behavioral chamber (Noldus Information Technology, Wageningen, the Netherlands) was used to assess free-swimming and startle behaviors under light conditions (100 % intensity ~4400 lx) at 25 frames per second. Experimental conditions were similar to those described previously (Tuz-Sasik et al., 2022). Briefly, individual larvae were, at 6 h post treatment (hpt), distributed in a checker-board fashion, control *versus* treated larvae, in a 48-well plate. Larvae were acclimatized inside the DanioVision chamber at 28 °C for 50 min in light. Each trial included a free-swimming episode for 10 min followed by a sequence of three taps, at 6-min intervals, to elicit startle responses. Taps were done at level 8 (most intense) for all experiments. At 24 hpt and 48 hpt, the behaviors of larvae were tested with the same experimental paradigm.

Larvae were tracked by Noldus EthoVision XT (version 13, Noldus Information Technology, Wageningen, the Netherlands). The following parameters were analyzed for free-swimming: total distance moved, maximum velocity, maximum acceleration, maximum deceleration, cumulative time accelerating, and number of accelerations. For startle responses, the following variables were analyzed over a period of 280 ms after each tap: total distance moved, maximum velocity, maximum acceleration, and cumulative time accelerating. An average of the three taps was used for analysis of each larvae.

All behavioral experiments were performed between 13.00 h and 19.00 h. Two independent trials were performed for each condition on different days from different parent fish.

2.8. In vivo imaging and time-lapse recordings

All imaging was performed using a Leica SP8 confocal microscope (Leica Microsystems, Wetzlar, Germany) using a 25× water objective. Larvae were mounted in low melting agarose (1.2 %) and kept anesthetized by Tricaine (0.12 mg/ml) during image acquisition. Leica's LasX software was used for image acquisition and processing. Time-lapse confocal images were taken at approximately 30-minute intervals.

2.9. Reanalyzing of single cell RNA-sequencing data from homeostatic and regenerating neuromasts

Previously published and publicly available single cell RNA-sequencing data (Baek et al., 2022) were used *via* a web-based interface (https://piotrowskilab.shinyapps.io/neuromast_regeneration_scRNAseq_pub_2021/). We searched the single cell database for expression of the following neurotrophins (Aragona et al., 2022; Nittoli et al., 2018): bdnf, ngf, ntf3, nt4/5, and nt6/7. We found that none of the neuromast components expressed nt4/5 or nt6/7, but we did find expression of bdnf, ngf, and ntf3. The dot plot was generated and downloaded.

2.10. Statistical analyses

Statistical analyses were performed using GraphPad Prism 9 for Windows (GraphPad Software, La Jolla, CA, USA). For all data, we first identified possible outliers with ROUT (Q = 0.1 %) and data were tested for normal distribution using a Kolmogorov-Smirnov test. When assumptions were fulfilled, unpaired *t*-tests (two-tailed) were performed to compare treated groups with untreated age-matched control groups. In the cases where the assumptions of normality were not fulfilled, a non-parametric Mann-Whitney-*U* test was applied. The level of significance was set at $p \leq 0.05$ (two-tailed) (* $p \leq 0.05$, ** $p \leq 0.01$, *** $p \leq 0.001$, **** $p \leq 0.0001$). Statistics for the behavioral parameters can be found in the supplementary Tables S1–3.

3. Results and discussion

3.1. Behavioral and anatomical recovery following hair cell ablation

It was shown that chemical ablation of hair cells by neomycin treatment alters swim behavior, including the startle response of zebrafish (Han et al., 2020; Newton et al., 2023; Suli et al., 2012; Tuz-Sasik et al., 2022). Here, we ablated hair cells and followed the behavioral recovery and linked this to the regeneration of hair cells, sensory afferent and inhibitory efferent projections (Fig. 1A). Ablations were performed at 5 dpf and behavioral recovery was monitored at 6, 24, and 48 h post treatment (hpt). In line with previous studies (Han et al., 2020; McHenry et al., 2009), parameters of free-swimming and startle response were significantly reduced at 6 hpt (Fig. 1B). Free-swimming behavior returned to control levels at 24 hpt, while the startle response recovered within 48 hpt (Fig. 1B, Tables S1–3).

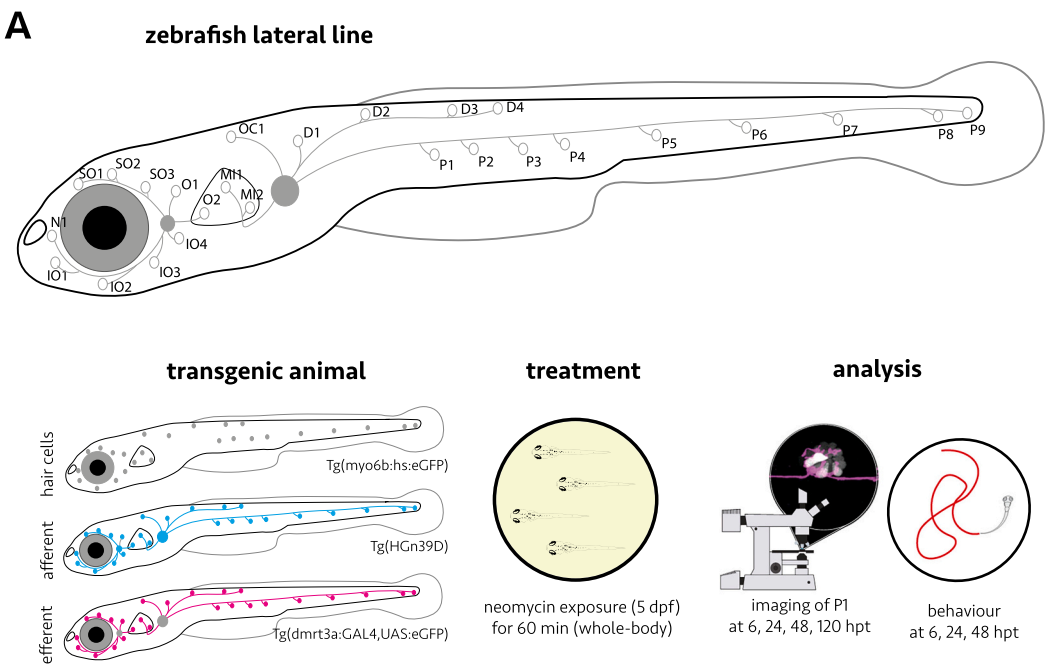

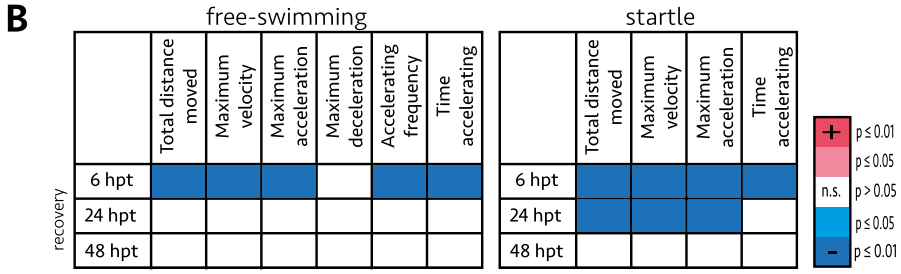

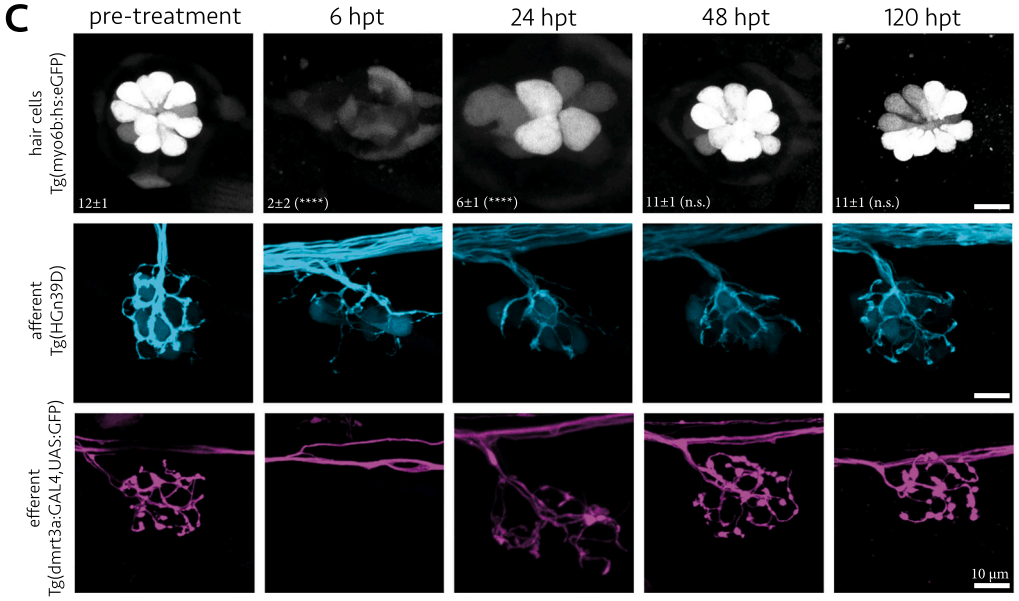

(caption on next page)

Fig. 1. Behavioral and anatomical analysis following hair cell ablation. A) Schematic overview of the experimental design. We used larvae from Tg(*myo6b*:hs:eGFP) labelling hair cells (white), Tg(HGn39D) labelling sensory afferent neurons (cyan), and Tg(*dmrt3a*:GAL4,UAS:eGFP) labelling inhibitory efferent neurons (magenta). At 5 dpf, larvae were exposed to neomycin (60 min, whole-body treatment) and analyzed for behavior at 6, 24, 48 h post treatment (hpt) as well as regeneration of anatomical components at the P1 neuromast at 6, 24, 48, 120 hpt. B) Swimming parameters analyzed were decreased (blue colour coded) following hair cell ablation (6 hpt), with free-swimming behavior returning to control conditions within 24 hpt, and the startle response within 48 hpt. We did not observe any parameters that were increased (red colour coded). C) The number of hair cells and innervation of sensory afferent and inhibitory efferent projections were strongly reduced at 6 hpt. The number of hair cells returned to control numbers at 48 hpt. Reinnervation by sensory afferent and inhibitory efferent projections took between 48 hpt and 120 hpt. Note that in some cases (2/5) we observed no inhibitory efferent projections at the P1 neuromast at 6 hpt. One-sample *t*-tests *versus* age-matched controls: 6hpt ($t = 13.69$, df = 5, $p < 0.0001$, ****); 24hpt ($t = 15.81$, df = 5, $p < 0.0001$, *****); 48hpt ($t = 2.000$, df = 5, $p = 0.10$, n.s.); 120hpt ($t = 2.236$, df = 5, $p = 0.08$, n.s.). (For interpretation of the references to colour in this figure legend, the reader is referred to the web version of this article.)

Next, we visualized the anatomical status of the lateral line following ablation by imaging hair cells using Tg(*myo6b*:hs:eGFP), sensory afferent projections using Tg(HGn39D) and inhibitory efferent projections using Tg(*dmrt3a*:GAL4;UAS:eGFP) at the P1 neuromast at 6, 24, 48, and 120 hpt (Figs. 1C; Figs. S1–S3). On average, control neuromasts contained 12 (±1) hair cells, and the majority of these were ablated at 6 hpt (2 ± 2 cells/neuromast; $n = 6$; $p < 0.0001$), with partial recovery at 24 hpt (6 ± 1 cells/neuromast; n = 6; $p < 0.0001$), and full recovery at 48 hpt (11 ± 1 cells/neuromast; n = 6; $p = 0.10$) and 120 hpt (11 ± 1cells/neuromast; n = 6; $p = 0.08$). The sensory afferent projections were visibly retracted at 6 hpt, but remained at the site of the neuromast (Fig. 1C). Reinnervation of neuromasts matched the regeneration of hair cells (24–120 hpt) and were in line with previous reports (Faucherre et al., 2009; Hardy et al., 2021; Jiang et al., 2014; Lush and Piotrowski, 2014). For the inhibitory efferent projections, we also observed reduced innervation, in line with the lack of hair cells and reduced sensory afferent innervation. Interestingly, we also observed cases with a complete absence of efferent projections at the site of the neuromast (Fig. 1C: 6 hpt, Fig. S3: 2/5 observations).

Mechanosensory activation of neuromast hair cells is crucial for proper free-swimming behavior (Desban et al., 2022). Our behavioral data suggests that free-swimming behavior requires only partial recovery of the lateral line system (*i.e.* lower number of hair cells, reduced innervation). It also suggests that activity of the regenerated hair cells is registered by the afferent neurons. Although it is unknown to what extent inhibitory modulation influences free-swimming behavior, it is likely that this is also partially recovered at 24 hpt, together with the other components of the network. Further recovery of the lateral line occurred within 48 hpt, signified by the behavioral recovery of the startle response and a full number of hair cells. Although the afferent and efferent innervation improved, additional recovery was observed between 48 hpt and 120 hpt. Regardless, a 48 hpt recovery period is in line with previous work, where synaptic refinement and neuronal connectivity in the regenerating lateral line require approximately 48 h to restore normal functionality (Hardy et al., 2021). Together, our behavioral analysis and imaging data suggest that demanding behaviors (*i.e.* startle response), where sensory inhibition may be more critical, require a more complete network.

3.2. Inhibitory efferent projections degenerate following hair cell ablation

To follow up on the absence of inhibitory efferent projections in some neuromasts following ablation, we performed time-lapse recordings of efferent projections at the P8-P9 neuromasts. We have previously shown that these neuromasts are innervated by a single inhibitory efferent subtype at 5 dpf (RELL cell; Manuel et al., 2021), which simplifies the analysis.

We crossed Tg(*myo6b*:hs:eGFP), to visualize hair cells, with Tg (*dmrt3a*:GAL4; UAS:Tomato), which labels the inhibitory efferent neurons in a mosaic manner, and selected for larvae that labelled a RELL neuron. After ablating the tail neuromasts (Fig. 2A), we recorded the fate of 27 RELL projections and found that in approximately half of the cases (15 of 27) the efferent axon degenerated within 12 hpt (average: 11h30min (±1h30min); Fig. 2B; Videos S1–S2). As inhibitory efferent projections connect directly to mature hair cells (Plazas and Elgoyhen, 2021), the hair cell loss is likely to be the cause for axonal degeneration.

Sensory afferent axons also synapse directly onto hair cells but are able to form connections to support cells within the neuromast following hair cell ablation (Hardy et al., 2021). To confirm that sensory afferent axons remained, we crossed Tg(*dmrt3a*:GAL4; UAS:Tomato) with Tg (HGn39D) and followed the fate of sensory projections of 10 larvae following hair cell ablation (Fig. 3A). No cases were observed where the sensory axons degenerated following ablation, including cases where the efferent RELL projection was lost (Figs. 3B, S4).

Next, we wondered if the efferent neuron survived or if the axon degeneration was a consequence of apoptosis. Through static imaging of larvae in which the RELL projection degenerated, we found that axon loss was restricted to the ablated region, *i.e.* neuromast P5-P9, while the axon and innervation was retained for unexposed neuromasts (Fig. 3C). Thus, the efferent neurons not only survived, but still had an axonal projection along the lateral line. Subsequent static imaging revealed that a growth cone emerges from the remaining RELL projection at 48 hpt, extending along the axonal tract of the lateral line, eventually reconnecting to the P8-P9 neuromasts at 120 hpt (Fig. 3C).

It should be noted, that we are looking at early stages during zebrafish development and therefore this process may be different in adults. Studies on neuromast regeneration in adult zebrafish have revealed that the regeneration process is slower in older animals, but still with full recovery (Cruz et al., 2015). Together with the regeneration of damaged neuromasts, new neuromasts are formed in juvenile and adult zebrafish (Ledent, 2002; Wada et al., 2013). These newly formed neuromasts are also innervated by afferent and efferent projections, suggesting the lateral line system maintains its regenerative powers throughout life. Thus, recovery and regeneration of efferent axons may well be similar in juvenile and adult zebrafish. Here, we show that while afferent axons remain in the neuromast, efferent axons are prone to degenerate following hair cell ablation, revealing a distinct difference in their response. However, in this model, the efferent axons are able to regenerate and reinnervate the newly formed hair cells.

3.3. Rapid hair cell regeneration potentially rescues efferent axons

Efferent projections seem to require hair cells for survival. If so, differences in efficiency of the neomycin treatment may explain why some degenerate and others remain. We quantified the number of hair cells immediately following ablation (1 hpt) and did not observe any DASPEI-labelled hair cells at the level of the P7-P9 neuromasts ($n = 10$ larvae), indicating that our ablation protocol efficiently ablates mature hair cells. In addition, we assessed hair cell numbers following DASPEI staining at 6 hpt. No DASPEI-labelled hair cells were observed where the efferent projection had degenerated (n = 1). In contrast, 1.75 (± 1.2) DASPEI-stained hair cells were found in cases where the RELL projection was retained ($n = 6$). This suggests that, in most neuromasts, mature hair cells were present again within 6 hpt. Such rapid formation of mature hair cells was also observed in previous work (Venuto and Erickson, 2021), where maturation of immature hair cells occurred between 1 and 5 h after ablation. Variables, such as sensitivity of individual immature hair cells to neomycin may differ between larvae and neuromasts, resulting in the ablation of immature hair cells in some cases. Moreover, even among immature hair cells that survived treatment, there could be

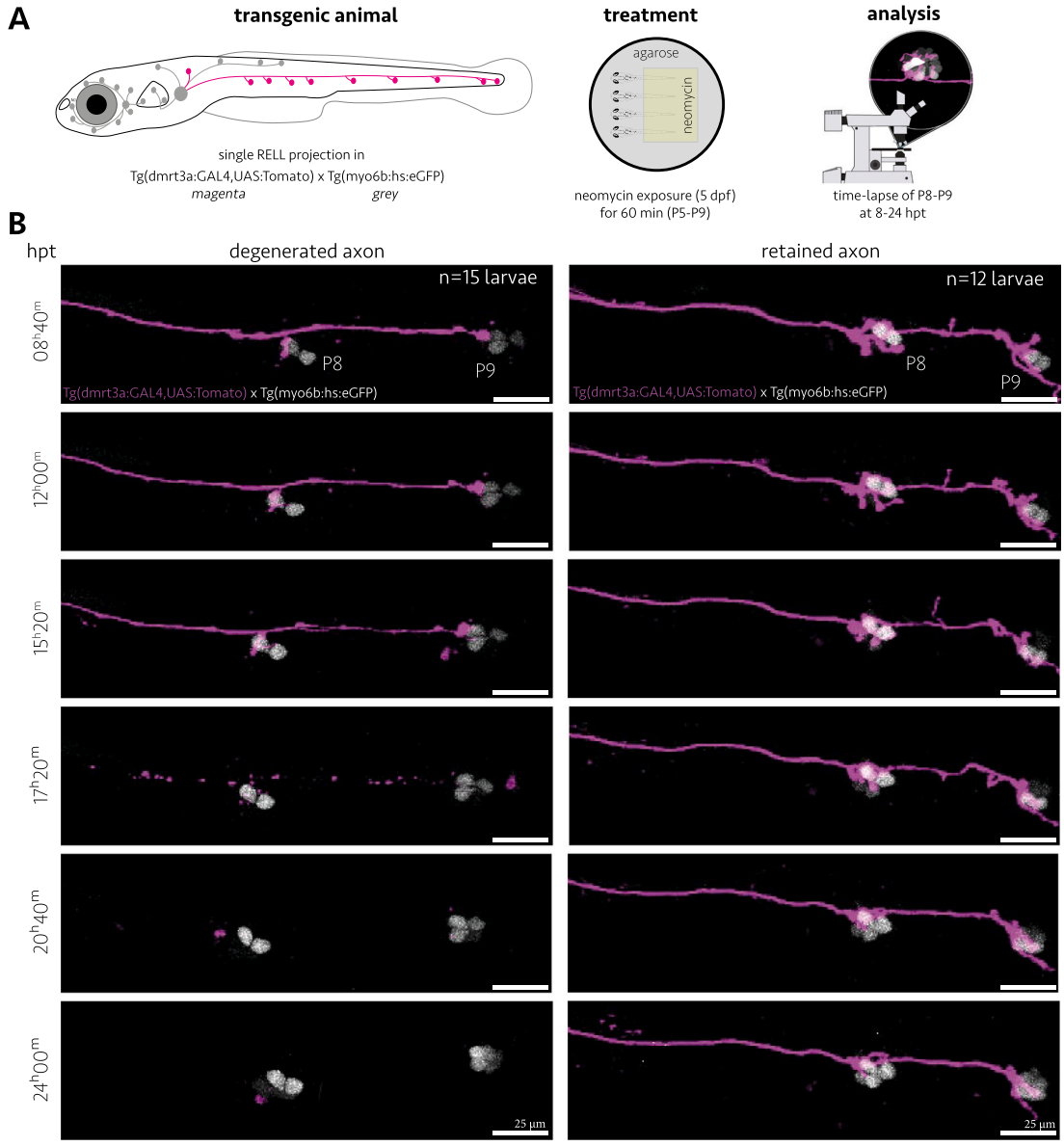

Fig. 2. Inhibitory efferent degeneration following hair cell ablation. A) Schematic overview of the experimental design. We used larvae from Tg(*dmrt3a*:GAL4,UAS:Tomato) labelling a single inhibitory efferent RELL neuron (magenta). At 5 dpf, larvae were exposed to neomycin (60 min, P5-P9 neuromasts) and time-lapse recordings were made of the P8-P9 neuromasts starting 3 h post treatment (hpt). B) We observed the fate of 27 RELL projections and found that in 15 cases the efferent projections degenerated (Video S1), while the other 12 efferent projections were retained (Video S2). (For interpretation of the references to colour in this figure legend, the reader is referred to the web version of this article.)

variation in how fast they mature, depending on their maturation state during, or the impact of, the neomycin treatment. The range over which we saw efferent axons degenerate suggests that there is a window where efferent axons may survive if new mature hair cells are formed fast enough.

3.4. Axon survival does not appear to be governed through the Bdnf/Trk-pathway

To reach a greater insight into the molecular mechanism, we reanalyzed previously published single cell RNA-sequencing data from homeostatic and regenerating neuromasts (Baek et al., 2022). We searched the single cell database for expression of the following neurotrophins (Aragona et al., 2022; Nittoli et al., 2018): *bdnf*, *ngf, ntf3, nt4/5,* and *nt6/7*. We found that none of the neuromast components expressed *nt4/5* or *nt6/7,* but we did find expression of *bdnf*, *ngf,* and *ntf3*. Although transcripts for *ngf* and *ntf3* were found in mature hair cells, young hair cells, and progenitor cells, their expression levels were consistently low both during homeostasis and throughout the regeneration process (Fig. 4A). Interestingly, *bdnf* is highly expressed in mature hair cells, but shows low expression levels in other cells of the neuromast, including the immature hair cells (Figs. 4A; see S5 for all neuromast cells). During regeneration of the neuromast, the number of young hair cells that express *bdnf* is increased (3–5 hpt) and expression levels increase in mature hair cells (5–10 hpt). As *bdnf* remains expressed during homeostasis of mature hair cells, the upregulation of *bdnf* during regeneration is likely a consequence of, rather than driving, the maturation process. However, it should be noted that Bdnf may have an autocrine function within the neuromast of zebrafish (Aragona et al., 2022). Previously, Bdnf was shown to be important for survival of cholinergic neurons (Morse et al., 1993), supporting the notion that Bdnf could also be responsible for the survival of the cholinergic efferent projections studied here (Bricaud

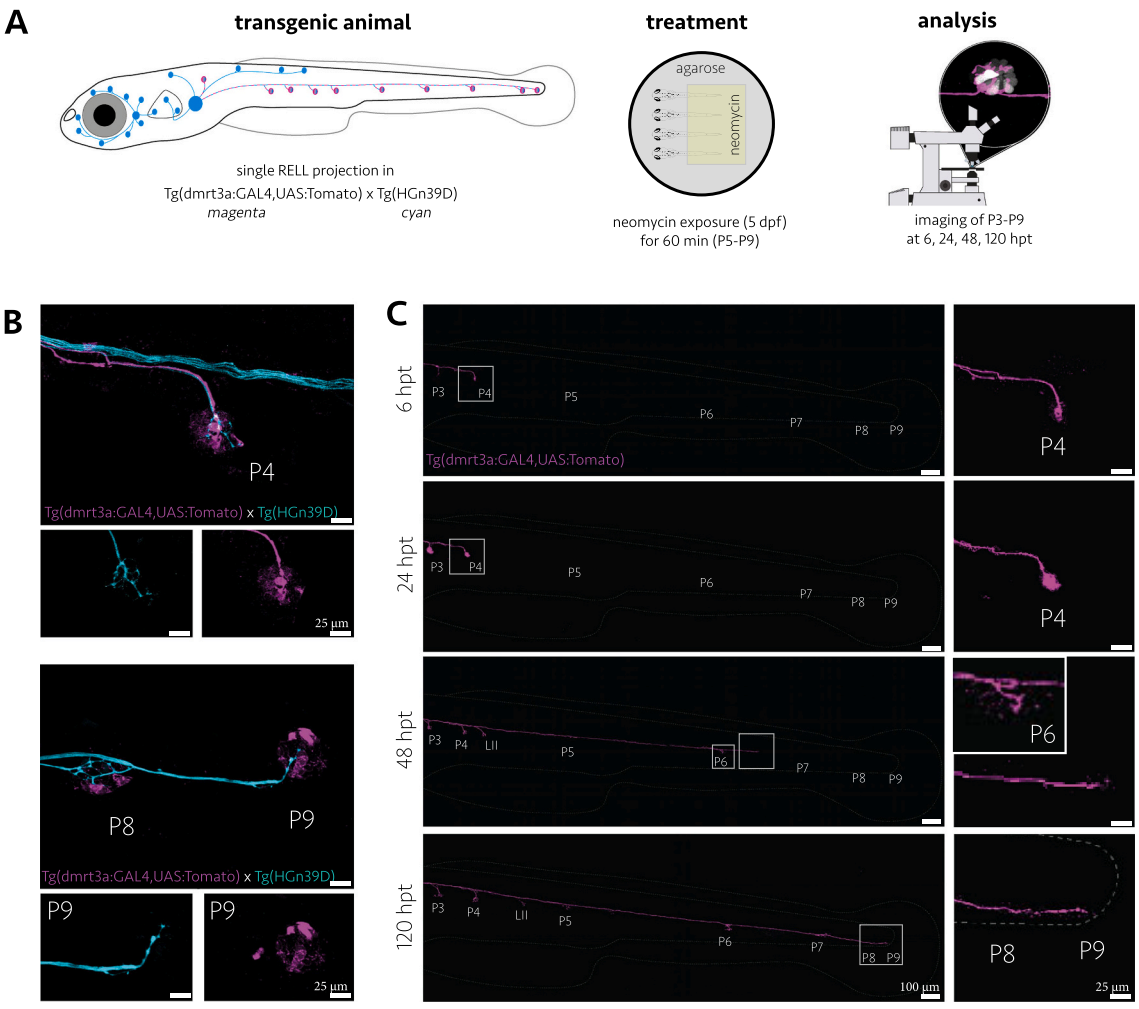

Fig. 3. Sensory afferent fate and inhibitory efferent regeneration following hair cell ablation. A) Schematic overview of the experimental design. We used larvae from a cross between Tg(HGn39D) and Tg(*dmrt3a*:GAL4,UAS:Tomato) labelling all sensory afferents (cyan) and a single inhibitory efferent RELL neuron (magenta). At 5 dpf, larvae were exposed to neomycin (60 min, P5-P9 neuromasts) and imaged at the P8-P9 neuromasts at 6, 24, 48, 120 h post treatment (hpt). B) Sensory projections remain at the site of the ablated neuromasts, even in cases where the inhibitory efferent projection degenerated. C) Following axonal degeneration of the inhibitory efferent, the retained portion of the axon started to migrate along the lateral line again within 48 hpt, innervating the regenerated P8-P9 neuromasts around 120 hpt. (For interpretation of the references to colour in this figure legend, the reader is referred to the web version of this article.)

et al., 2001; Flock and Russell, 1973). To test this idea, we exposed larvae to a Bdnf antibody (Wright and Ribera, 2010) in order to block the action of Bdnf, and assessed whether efferent projections degenerated as a result (Fig. 4B). We observed the fate of 9 RELL projections following a 24 h-treatment with Bdnf antibodies, and found no signs of degeneration. In addition, we did not observe notable changes in the level of neuromast innervation (Fig. 4C). To corroborate our observations, along with exploring a role for Ngf and Ntf3 as survival factors, we decided to block all three neurotrophin receptors (TrkA, TrkB, and TrkC; Skerratt et al., 2016). Here, Bdnf binds to TrkB, while Ngf show preferential binding to TrkA and Ntf3 to TrkC (Reichardt, 2006; Skaper, 2012). Furthermore, we inhibited the ERK-pathway, which is known to act downstream of these receptors (Skaper, 2012). We observed 6 (TrK) and 4 (ErK) treated RELL cells, but saw no degeneration of their projections following 24 h of exposure (Fig. 4D). While we have used similar concentrations and protocols as previous studies (Hawkins et al., 2008; Uribe et al., 2015; Wright and Ribera, 2010), and amended them to our experimental approach, we cannot guarantee the effectiveness of the aimed blocking. However, we used three strategies to target Bdnf signaling at different levels: sequestering Bdnf itself, blocking the receptor, and inhibiting the downstream signaling pathway. Moreover, the superficial positioning of the neuromasts, together with the 24 h incubation period, should allow for adequate exposure and penetrance by the substances used. Therefore, we are confident in our statement that it is very unlikely that survival of efferent projections relies on the presence of Bdnf. Here, we looked at the role of Bndf as a survival cue, but in mammals, BDNF has been reported to promote axonal regeneration within the cochlea following injury (Altschuler et al., 1999). The dynamic expression of *bdnf* in the neuromast cells during regeneration could thus be linked to the innervation processes, rather than the survival of efferent axons. Single cell sequencing of efferent neurons would provide information regarding the receptors these cells express and thereby offer a new approach to identify the survival mechanism involved.

3.5. *Inhibitory efferent projections still exist in larvae void of mature hair cells*

Although survival of efferent projections does not appear to rely on neurotrophins, they do seem reliant on mature hair cells. With that in mind, we asked what would happen to the inhibitory efferent neurons if there were a complete lack of mature hair cells. To this end, we generated *atoh1a* crispant Tg(*dmrt3a*:GAL4,UAS:eGFP) larvae, where hair cells fail to mature in the absence of atoh1a (Navajas Acedo et al., 2019),

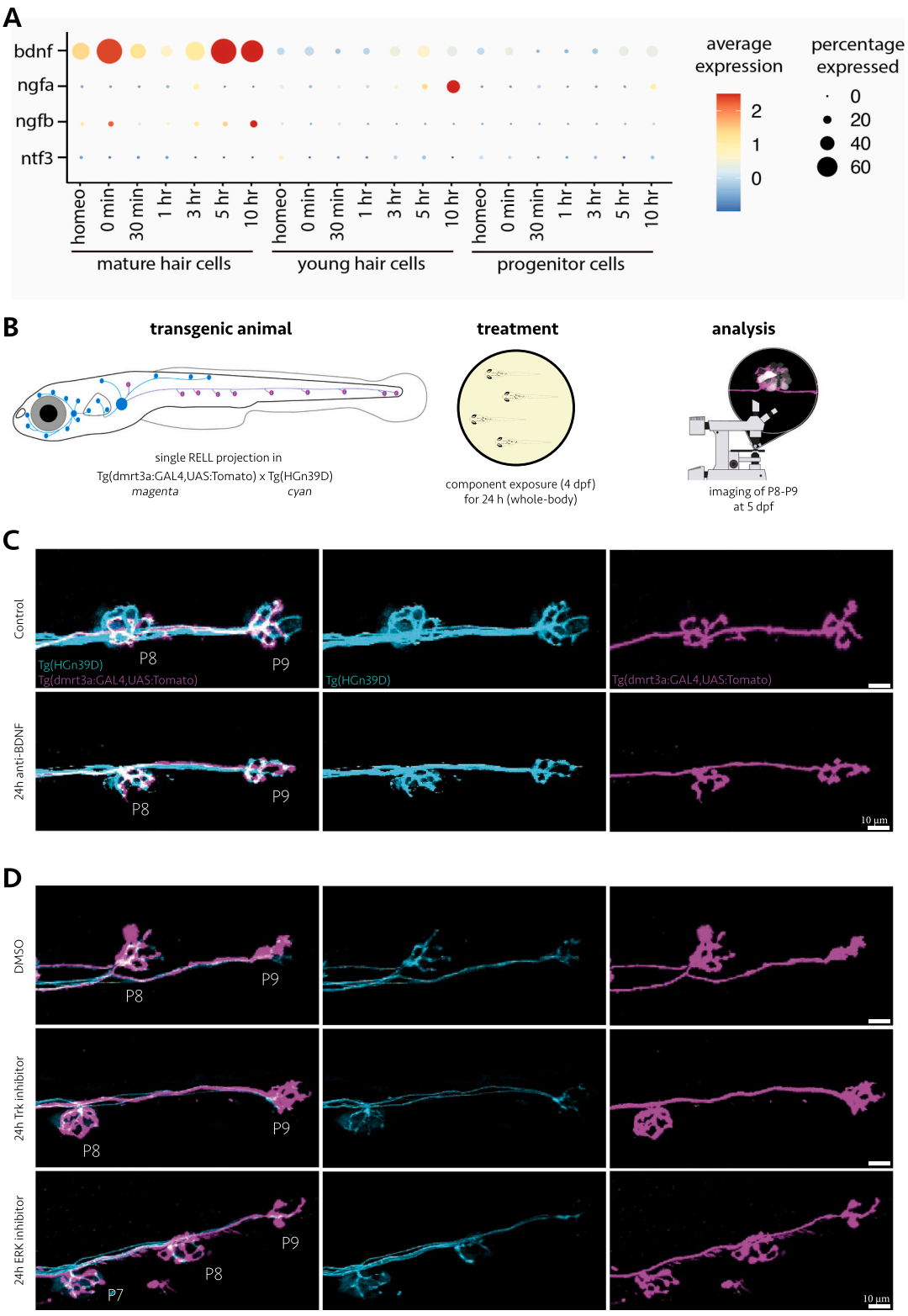

Fig. 4. Bdnf expression in neuromast cells during homeostasis and regeneration. A) Expression of *ngfa*, *ngfb*, and *ntf3* was low in mature and young (immature) hair cells, and progenitor cells during homeostasis and regeneration of the neuromast. In contrast, expression of *bdnf* was more dynamic: during homeostasis, expression in mature hair cells (0 to +1 *average expression*), was higher than that in young hair cells (0 to −1) and progenitor cells (0 to −1). During regeneration expression in mature hair cells increases, reaching peak expression at 5 hpt (over +2) and 10 hpt (over +2). For young hair cells, more cells expressed *bdnf* and expression levels increased for 3 hpt and 5 hpt (0 to +1). The size of the dots represents the proportion of cells expressing the gene. B) Schematic overview of the experimental design. We used larvae from a cross between Tg(HGn39D) and Tg(dmrt3:GAL4,UAS:Tomato) labelling all sensory afferents (cyan) and a single inhibitory efferent RELL neuron (magenta). C) Overnight exposure to anti-BDNF antibodies did not induce degeneration of efferent axons ($n = 9$ RELL axons). D) Overnight exposure to Trk-receptor blockers ($n = 6$ RELL axons) or ERK-pathway inhibitors ($n = 4$ RELL axons) did not result in efferent axon degeneration. Fig. A was generated through data made available by Piotrowski Lab (Baek et al., 2022): https://piotrowskilab.shinyapps.io/neuromast_regeneration_scRNAseq_pub_2021.

and assessed the efferent projections along the lateral line (Fig. 5A). We screened 5-day old F0 larvae by staining neuromast hair cells with DASPEI (Fig. 5B). We found that 1 out of 60 larvae completely lacked hair cells, while 8/60 displayed a mosaic pattern of hair cell loss (Fig. 5C). Imaging *atoh1a* mutant larvae that completely lack neuromast hair cells, revealed that inhibitory efferent neurons were still present and sent out projections to the lateral line (8 dpf, Fig. 5C'). Here, efferent neurons had projections along the lateral line tract comparable to controls, with collaterals extending to the neuromasts. However, at the neuromast, efferent projections lingered at the 'base' and did not innervate the hair cell, as judged by the absence of branching and synaptic buttons (Fig. 5C″). The presence of efferent projections along the

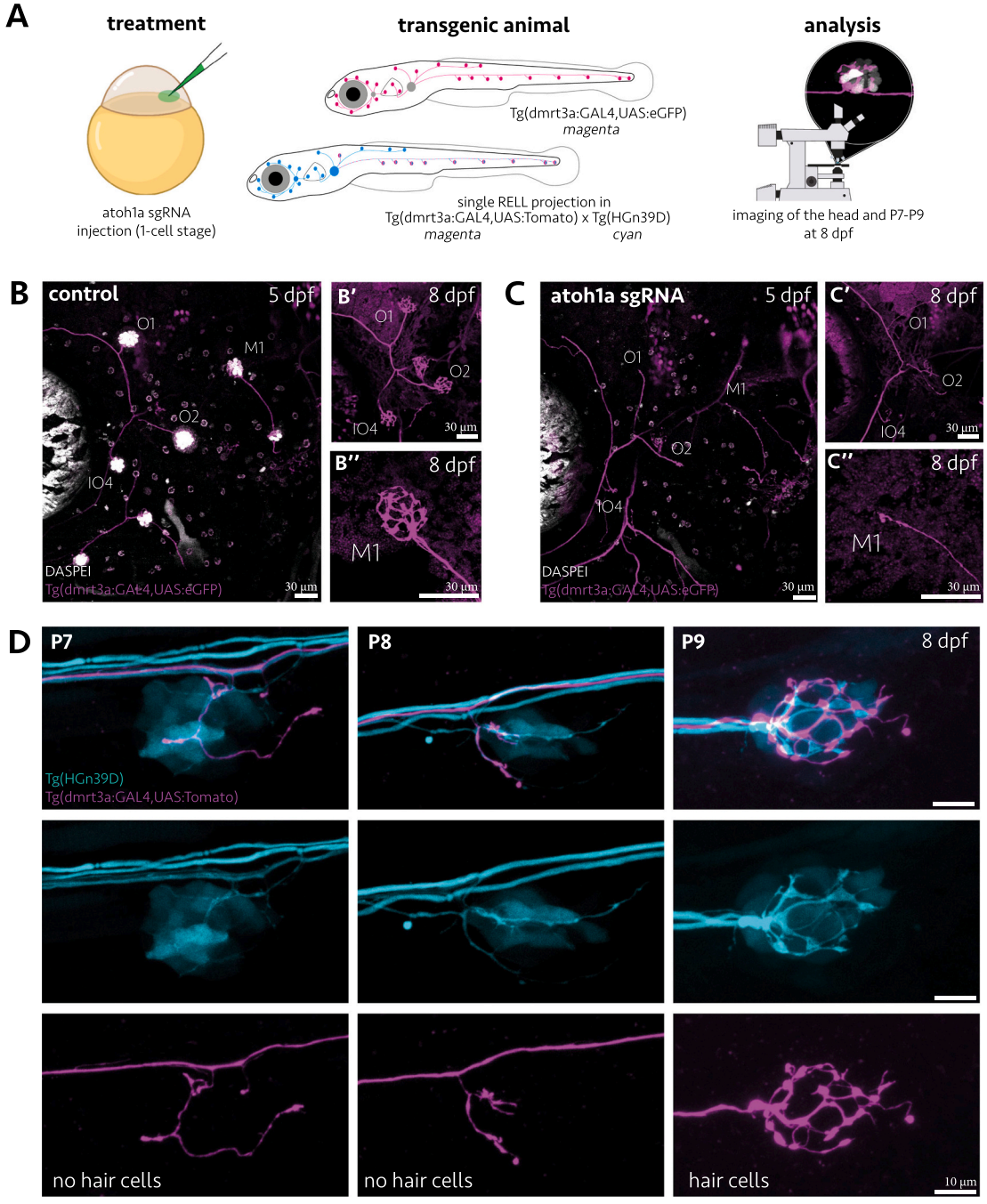

Fig. 5. Inhibitory efferent degeneration in the absence of hair cell formation. A) Schematic overview of the experimental design. We used larvae from Tg(*dmrt3a*:GAL4,UAS:eGFP) labelling the inhibitory efferent neurons (magenta) as well as the larvae from a cross between Tg(HGn39D) and Tg(*dmrt3a*:GAL4,UAS:Tomato) labelling all sensory afferents (cyan) and a single inhibitory efferent RELL neuron (magenta). At the 1-cell stage, embryos were injected with *atoh1a* sgRNAs in order to generate crispant knock-out for the *atoh1a* gene. B-C) Examples of a control larvae (B), showing hair cells following DASPEI staining (white) and an *atoh1a* crispant larvae (C) lacking DASPEI-stained hair cells (5 dpf). B′-C′) Zoomed image of the O1, O2, and IO4 neuromasts 3 days later (8 dpf) for the same larvae, but now without DASPEI staining for a cleaner image. B″-C″) A higher magnification image of the M1 neuromast at 8 dpf, detailing efferent axon innervation of the neuromast organ in control larvae, but not so in *atoh1a* crispant larvae. D) Detailed images of the P7-P9 neuromasts of a Tg(HGn39D, *dmrt3a*:GAL4:UAS:Tomato) *atoh1a* crispant larvae (8 dpf), labelling both the sensory afferents (cyan) and a RELL projection (magenta). Earlier DASPEI staining (5 dpf) revealed a lack of hair cells for the P7 and P8 neuromast, but we identified hair cells for the P9 neuromast (Fig. S6). (For interpretation of the references to colour in this figure legend, the reader is referred to the web version of this article.)

lateral line in *atoh1a* crispants, suggests that the efferent axon survival only becomes dependent on mature hair cells after their initial synaptic contact. In the absence of hair cells, efferent axons likely remain in a 'seek'-state where they continue to search for mature hair cells to innervate. At this point, it is unclear how long efferent neurons would continue seeking neuromasts. Generally, the ability of neurons to reach their target is essential for their survival (Bean, 1997), but as the number of neuromasts of the lateral line increases throughout the lifespan of the zebrafish, it is possible that the capacity of the efferent neurons to innervate new targets would remain into adulthood.

In addition, the innervation of neuromasts (or lack thereof) by sensory afferent neurons were comparable to that of the efferent axons in *atoh1a* crispants (Fig. 5D), indicating that they also require mature hair cells for proper innervation of the neuromast organ. This is illustrated in a mosaic patterned *atoh1a* crispant larvae, where DASPEI staining revealed hair cells in the P9 neuromast, but a lack thereof in the P8 and P7 neuromast (Figs. 5D, S6). Here, the innervation of the P9 neuromast is normal, while the P7 and P8 show reduced innervation, with projections protruding out, likely in search of hair cells.

Conclusion and future perspectives

For the first time, we bring insights into the fate of the inhibitory efferent projections during ablation and regeneration of the lateral line hair cells in zebrafish. Once synaptic connectivity has been established, the survival of efferent axons becomes dependent on the presence of mature hair cells in the neuromast. Following the loss of mature hair cells, rapid formation of mature hair cells during the regeneration process can prevent axonal degeneration. Although *bdnf* is dynamically expressed during the regeneration of the neuromast, survival of efferent axons does not appear to be reliant on Bdnf or any of the other neurotrophic factors.

In mammals, cochlear hair cells are also innervated by efferent fibers (Plazas and Elgoyhen, 2021). Specifically, the cholinergic medial olivocochlear (MOC) fibers, which make direct contact with outer hair cells (Warr et al., 1997), show profound similarity with the inhibitory efferent projections we studied here. This stresses the importance of also addressing the efferent innervation in a mammalian context. Given the reduced regenerative ability of the mammalian central nervous system neurons, we hope that our data will lead to new studies in the pursuit of treatments of hearing defects, specifically those related to faulty efferent modulation in humans. In a larger perspective, efferent modulation is likely a key aspect of multiple sensory systems, highlighting the need to better understand and take this component into consideration.

Supplementary data to this article can be found online at https://doi.org/10.1016/j.mcn.2023.103900.

Funding

This work was supported by Swedish Research Council (2020-03365), Ragnar Söderberg Foundation (1235/17), Hjärnfonden (FO2020-0129) and Swedish Foundation for Strategic Research (FFL18-0112). The author RM was supported by Olle Engkvists Stiftelse (204-0243) and the author MUT-S was supported by Hjärnfonden (FO2020-0129).

CRediT authorship contribution statement

Melek Umay Tuz-Sasik: Conceptualization, Data curation, Formal analysis, Investigation, Methodology, Writing-original draft. **Remy Manuel:** Conceptualization, Funding acquisition, Methodology, Project administration, Supervision, Visualization, Writing – review & editing. **Henrik Boije:** Conceptualization, Funding acquisition, Methodology, Resources, Supervision, Writing – review & editing.

Declaration of competing interest

The authors have declared that no competing interests exists.

Data availability

Data will be made available on request.

Acknowledgements

We thank the Genome Engineering Zebrafish National Facility (Uppsala, Sweden) for fish husbandry. We also thank Judith Habicher for designing *myo6b* sgRNA used to generate Tg(*myo6b*:hs:eGFP). The drawing of the Confocal Microscope (https://doi.org/10.5281/zenodo.4421181) used in our figures, was made by Alexander Bates and freely available from SciDraw (https://scidraw.io).

References

Akitake, C.M., Macurak, M., Halpern, M.E., Goll, M.G., 2011. Transgenerational analysis of transcriptional silencing in zebrafish. Dev. Biol. 352, 191–201.

Altschuler, R.A., Cho, Y., Ylikoski, J., Pirvola, U., Magal, E., Miller, J.M., 1999. Rescue and regrowth of sensory nerves following deafferentation by neurotrophic factors. Ann. N. Y. Acad. Sci. 884, 305–311. https://doi.org/10.1111/j.1749-6632.1999.tb08650.x.

Aragona, M., Porcino, C., Guerrera, M.C., Montalbano, G., Laurà, R., Cometa, M., Levanti, M., Abbate, F., Cobo, T., Capitelli, G., Vega, J.A., Germanà, A., 2022. The BDNF/TrkB Neurotrophin system in the sensory organs of zebrafish. Int. J. Mol. Sci. 23, 2621. https://doi.org/10.3390/ijms23052621.

Baek, S., Tran, N.T.T., Diaz, D.C., Tsai, Y.Y., Acedo, J.N., Lush, M.E., Piotrowski, T., 2022. Single-cell transcriptome analysis reveals three sequential phases of gene expression during zebrafish sensory hair cell regeneration. Dev. Cell 57, 799-819.e6. https://doi.org/10.1016/j.devcel.2022.03.001.

Bean, A., 1997. Chapter 9: Synapse Formation, Survival, and Elimination. In: Byrne, J.H. (Ed.), Neuroscience Online: An Electronic Textbook for the Neurosciences. Department of Neurobiology and Anatomy McGovern Medical School at The University of Texas Health Science Center at Houston (UTHealth).

Bricaud, O., Chaar, V., Dambly-Chaudière, C., Ghysen, A., 2001. Early efferent innervation of the zebrafish lateral line. J. Comp. Neurol. 434, 253–261. https://doi.org/10.1002/cne.1175.

Coffin, A.B., Ou, H., Owens, K.N., Santos, F., Simon, J.A., Rubel, E.W., Raible, D.W., 2010. Chemical screening for hair cell loss and protection in the zebrafish lateral line. Zebrafish 7, 3–11. https://doi.org/10.1089/zeb.2009.0639.

Cruz, I.A., Kappedal, R., Mackenzie, S.M., Hailey, D.W., Hoffman, T.L., Schilling, T.F., Raible, D.W., 2015. Robust regeneration of adult zebrafish lateral line hair cells reflects continued precursor pool maintenance. Dev. Biol. 402, 229–238. https://doi.org/10.1016/j.ydbio.2015.03.019.

Desban, L., Roussel, J., Mirat, O., Lejeune, F.-X., Keiser, L., Michalski, N.A., Wyart, C., 2022. Lateral line hair cells integrate mechanical and chemical cues to orient navigation. bioRxiv 2022.08.31.505989.

Faucherre, A., Pujol-Martí, J., Kawakami, K., López-Schier, H., 2009. Afferent neurons of the zebrafish lateral line are strict selectors of hair-cell orientation. PloS One 4. https://doi.org/10.1371/journal.pone.0004477.

Flock, Å., Russell, I.J., 1973. The post-synaptic action of efferent fibres in the lateral line organ of the burbot Lota lota. J. Physiol. 235, 591–605. https://doi.org/10.1113/jphysiol.1973.sp010406.

Ghysen, A., Dambly-Chaudière, C., 2004. Development of the zebrafish lateral line. Curr. Opin. Neurobiol. 14, 67–73. https://doi.org/10.1016/j.conb.2004.01.012.

Han, E., Ho Oh, K., Park, S., Chan Rah, Y., Park, H.-C., Koun, S., Choi, J., 2020. Analysis of behavioral changes in zebrafish (Danio rerio) larvae caused by aminoglycoside-induced damage to the lateral line and muscles. Neurotoxicology 78, 134–142. https://doi.org/10.1016/j.neuro.2020.03.005.

Hardy, K., Amariutei, A.E., De Faveri, F., Hendry, A., Marcotti, W., Ceriani, F., 2021. Functional development and regeneration of hair cells in the zebrafish lateral line. J. Physiol. 599, 3913–3936. https://doi.org/10.1113/JP281522.

Harris, J.A., Cheng, A.G., Cunningham, L.L., MacDonald, G., Raible, D.W., Rubel, E.W., 2003. Neomycin-induced hair cell death and rapid regeneration in the lateral line of zebrafish (Danio rerio). JARO - J. Assoc. Res. Otolaryngol. 4, 219–234. https://doi.org/10.1007/s10162-002-3022-x.

Hawkins, T.A., Cavodeassi, F., Erdélyi, F., Szabó, G., Lele, Z., 2008. The small molecule Mek1/2 inhibitor U0126 disrupts the chordamesoderm to notochord transition in zebrafish. BMC Dev. Biol. 8, 42. https://doi.org/10.1186/1471-213X-8-42.

Jiang, L., Romero-Carvajal, A., Haug, J.S., Seidel, C.W., Piotrowski, T., 2014. Gene-expression analysis of hair cell regeneration in the zebrafish lateral line. Proc. Natl. Acad. Sci. U. S. A. 111 https://doi.org/10.1073/pnas.1402898111.

Kimura, Y., Hisano, Y., Kawahara, A., Higashijima, S., 2014. Efficient generation of knock-in transgenic zebrafish carrying reporter/driver genes by CRISPR/Cas9-mediated genome engineering. Sci. Rep. 4, 6545. https://doi.org/10.1038/srep06545.

Ledent, V., 2002. Postembryonic development of the posterior lateral line in zebrafish. Development 129, 597–604. https://doi.org/10.1242/dev.129.3.597.
Lush, M.E., Piotrowski, T., 2014. Sensory hair cell regeneration in the zebrafish lateral line. Dev. Dyn. 243, 1187–1202. https://doi.org/10.1002/dvdy.24167.
Manuel, R., Iglesias Gonzalez, A.B., Habicher, J., Koning, H.K., Boije, H., 2021. Characterization of individual projections reveal that neuromasts of the zebrafish lateral line are innervated by multiple inhibitory efferent cells. Front. Neuroanat. 15, 1–13. https://doi.org/10.3389/fnana.2021.666109.
McHenry, M.J., Feitl, K.E., Strother, J.A., Van Trump, W.J., 2009. Larval zebrafish rapidly sense the water flow of a predator's strike. Biol. Lett. 5, 477–479. https://doi.org/10.1098/rsbl.2009.0048.
Morse, J., Wiegand, S., Anderson, K., You, Y., Cai, N., Carnahan, J., Miller, J., DiStefano, P., Altar, C., Lindsay, R., 1993. Brain-derived neurotrophic factor (BDNF) prevents the degeneration of medial septal cholinergic neurons following fimbria transection. J. Neurosci. 13, 4146–4156. https://doi.org/10.1523/JNEUROSCI.13-10-04146.1993.
Navajas Acedo, J., Voas, M.G., Alexander, R., Woolley, T., Unruh, J.R., Li, H., Moens, C., Piotrowski, T., 2019. PCP and Wnt pathway components act in parallel during zebrafish mechanosensory hair cell orientation. Nat. Commun. 10, 3993. https://doi.org/10.1038/s41467-019-12005-y.
Newton, K.C., Kacev, D., Nilsson, S.R.O., Saettele, A.L., Golden, S.A., Sheets, L., 2023. Lateral line ablation by ototoxic compounds results in distinct rheotaxis profiles in larval zebrafish. Commun. Biol. 6, 84. https://doi.org/10.1038/s42003-023-04449-2.
Nittoli, V., Sepe, R.M., Coppola, U., D'Agostino, Y., De Felice, E., Palladino, A., Vassalli, Q.A., Locascio, A., Ristoratore, F., Spagnuolo, A., D'Aniello, S., Sordino, P., 2018. A comprehensive analysis of neurotrophins and neurotrophin tyrosine kinase receptors expression during development of zebrafish. J. Comp. Neurol. 526, 1057–1072. https://doi.org/10.1002/cne.24391.
Ota, S., Taimatsu, K., Yanagi, K., Namiki, T., Ohga, R., Higashijima, S., Kawahara, A., 2016. Functional visualization and disruption of targeted genes using CRISPR/Cas9-mediated eGFP reporter integration in zebrafish. Sci. Rep. 6, 34991. https://doi.org/10.1038/srep34991.
Ou, H.C., Santos, F., Raible, D.W., Simon, J.A., Rubel, E.W., 2010. Drug screening for hearing loss: using the zebrafish lateral line to screen for drugs that prevent and cause hearing loss. Drug Discov. Today 15, 265–271. https://doi.org/10.1016/j.drudis.2010.01.001.
Pichler, P., Lagnado, L., 2019. The transfer characteristics of hair cells encoding mechanical stimuli in the lateral line of zebrafish. J. Neurosci. 39, 112–124. https://doi.org/10.1523/JNEUROSCI.1472-18.2018.
Plazas, P.V., Elgoyhen, A.B., 2021. The cholinergic lateral line efferent synapse: structural, functional and molecular similarities with those of the cochlea. Front. Cell. Neurosci. 15, 1–15. https://doi.org/10.3389/fncel.2021.765083.
Pleasure, D., 1999. Regeneration in the central and peripheral nervous systems. In: Siegel, G.J., Agranoff, B.W., Albers, R.W., et al. (Eds.), Basic Neurochemistry: Molecular, Cellular and Medical Aspects. Lippincott-Raven, Philadelphia.
Reichardt, L.F., 2006. Neurotrophin-regulated signalling pathways. Philos. Trans. R. Soc. B Biol. Sci. 361, 1545–1564. https://doi.org/10.1098/rstb.2006.1894.
Satou, C., Sugioka, T., Uemura, Y., Shimazaki, T., Zmarz, P., Kimura, Y., Higashijima, S., 2020. Functional diversity of glycinergic commissural inhibitory neurons in larval zebrafish. Cell Rep. 30, 3036–3050.e4.
Skaper, S.D., 2012. In: Skaper, S.D. (Ed.), The neurotrophin Family of Neurotrophic Factors: An Overview. Humana Press, Totowa, NJ, pp. 1–12. https://doi.org/10.1007/978-1-61779-536-7_1.
Skerratt, S.E., Andrews, M., Bagal, S.K., Bilsland, J., Brown, D., Bungay, P.J., Cole, S., Gibson, K.R., Jones, R., Morao, I., Nedderman, A., Omoto, K., Robinson, C., Ryckmans, T., Skinner, K., Stupple, P., Waldron, G., 2016. The discovery of a potent, selective, and peripherally restricted Pan-Trk inhibitor (PF-06273340) for the treatment of pain. J. Med. Chem. 59, 10084–10099. https://doi.org/10.1021/acs.jmedchem.6b00850.
Suli, A., Watson, G.M., Rubel, E.W., Raible, D.W., 2012. Rheotaxis in larval zebrafish is mediated by lateral line mechanosensory hair cells. PloS One 7, e29727. https://doi.org/10.1371/journal.pone.0029727.
Tsonis, P.A., 2000. Regeneration in vertebrates. Dev. Biol. 221, 273–284. https://doi.org/10.1006/dbio.2000.9667.
Tuz-Sasik, M.U., Boije, H., Manuel, R., 2022. Characterization of locomotor phenotypes in zebrafish larvae requires testing under both light and dark conditions. PloS One 17, e0266491. https://doi.org/10.1371/journal.pone.0266491.
Uribe, P.M., Kawas, L.H., Harding, J.W., Coffin, A.B., 2015. Hepatocyte growth factor mimetic protects lateral line hair cells from aminoglycoside exposure. Front. Cell. Neurosci. 9, 1–10. https://doi.org/10.3389/fncel.2015.00003.
Vanwalleghem, G., Schuster, K., Taylor, M.A., Favre-Bulle, I.A., Scott, E.K., 2020. Brain-wide mapping of water flow perception in zebrafish. J. Neurosci. 40, 4130–4144. https://doi.org/10.1523/JNEUROSCI.0049-20.2020.
Varshney, G.K., Pei, W., LaFave, M.C., Idol, J., Xu, L., Gallardo, V., Carrington, B., Bishop, K., Jones, M., Li, M., Harper, U., Huang, S.C., Prakash, A., Chen, W., Sood, R., Ledin, J., Burgess, S.M., 2015. High-throughput gene targeting and phenotyping in zebrafish using CRISPR/Cas9. Genome Res. 25, 1030–1042. https://doi.org/10.1101/gr.186379.114.
Venuto, A., Erickson, T., 2021. Evaluating the death and recovery of lateral line hair cells following repeated neomycin treatments. Life 11, 1180. https://doi.org/10.3390/life11111180.
Wada, H., Dambly-Chaudière, C., Kawakami, K., Ghysen, A., 2013. Innervation is required for sense organ development in the lateral line system of adult zebrafish. Proc. Natl. Acad. Sci. 110, 5659–5664. https://doi.org/10.1073/pnas.1214004110.
Warr, W.B., Beck Boche, J., Neely, S.T., 1997. Efferent innervation of the inner hair cell region: origins and terminations of two lateral olivocochlear systems. Hear. Res. 108, 89–111. https://doi.org/10.1016/S0378-5955(97)00044-0.
Whitfield, T.T., 2002. Zebrafish as a model for hearing and deafness. J. Neurobiol. 53, 157–171. https://doi.org/10.1002/neu.10123.
Wright, M.A., Ribera, A.B., 2010. Brain-derived neurotrophic factor mediates non-cell-autonomous regulation of sensory neuron position and identity. J. Neurosci. 30, 14513–14521. https://doi.org/10.1523/JNEUROSCI.4025-10.2010.